arXiv:1609.08719v1 [math.GT] 28 Sep 2016

AN EXPERIMENTAL INVESTIGATION OF NEUMANN'S CONJECTURE

STEPHEN GILLES AND PETER HUSTON

Abstract. We use a large census of hyperbolic 3-manifolds to experimentally investigate a conjecture of Neumann regarding the Bloch Group. We present an augmented census including, for feasible invariant trace fields, explicit manifolds (associated to that field) that appear to generate the Bloch group of that field. We also make use of Ptolemy coordinates to compute "exotic volumes" of representations, and attempt to realize these volumes as linear combinations of generator volumes. We thus present a large body of empirical support for Neumann's conjecture.

Contents

1. Introduction 2
1.1. Neumann's conjecture 2
1.2. Neumann's weaker conjecture 2
1.3. A stronger, false conjecture 2
1.4. Exotic volumes 2
Acknowledgments 3
2. Background 3
2.1. Cross-ratios 3
2.2. The invariant trace field 3
2.3. The Bloch group 4
2.4. Gluing Equations 4
2.5. Ptolemy coordinates 7
2.6. Lattice matching 8
3. Experimentation 10
3.1. Manifold generation 10
3.2. Lattice matching 11
3.3. Linear combinations for exotic volumes 11
4. A counter-example to conjecture 1.3 11
5. Evidence for conjecture 1.2 12
5.1. Examples of missing fields 12
5.2. Data analysis 12
6. Selected examples 14
References 17

Date: 2016-09-17.

2010 *Mathematics Subject Classification.* 57N10 (primary), and 57M27 (secondary).

This work was supported in part by the National Science Foundation through the Research Experiences for Undergraduates (DMS# 1359307) at the University of Maryland, College Park.

1. Introduction

Our primary result, described in section 3, is a large census of hyperbolic 3-manifolds, organized by invariant trace field, together with tables expressing volumes as linear combinations of other manifolds' volumes. This census is available at `http://www.curve.unhyperbolic.org/linComb`. Examining this census has allowed us, in many cases, to explicitly list manifolds which give rise to elements in the Bloch groups of certain invariant trace fields that span all the elements of that Bloch group we observed, supporting a conjecture of Neumann.

1.1. **Neumann's conjecture.** For a hyperbolic 3-manifold M, we denote the element it induces in the Bloch Group (see section 2.3) as $[M]$. The conjecture we primarily studied was given in [Neu11], and stated in this form by [GTZ15]:

Conjecture 1.1 (Neumann)**.** *Let $F \subset \mathbb{C}$ be a number field not contained in $\mathbb{R}$, and let $\mathcal{M}$ be the set of manifolds with invariant trace fields contained in F,*

$$\mathcal{M} := \{M \cong \mathbb{H}^3/\Gamma \mid \mathbb{Q}(\operatorname{tr}\Gamma^{(2)}) \subseteq F\}.$$

Let $\mathcal{N} = \{[M] \mid M \in \mathcal{M}\}$ be elements of the Bloch group determined by manifolds in $\mathcal{M}$ (see section 2.3). Then integral combinations of elements of $\mathcal{N}$ generate $\mathcal{B}(F)$.

1.2. **Neumann's weaker conjecture.** Neumann has also proposed a weaker conjecture which our results also support.

Conjecture 1.2 ([Neu11, Conjecture 1])**.** *Every non-real concrete number field k arises as the invariant trace field of some hyperbolic manifold.*

In full form, this conjecture also addresses quaternion algebras, but we only examine invariant trace fields. Relevant results are discussed in section 5.

1.3. **A stronger, false conjecture.** We also considered whether conjecture 1.1 could be strengthened somewhat to the following form, which directly regards volumes of manifolds rather than Bloch group elements.

Conjecture 1.3. *Let $F \subset \mathbb{C}$ be a number field not contained in $\mathbb{R}$.*

Let $S = \{\operatorname{vol}(M) \mid M$ a hyperbolic 3-manifold with invariant trace field $F\}$. The lattice generated by S is linearly spanned by some $\{\operatorname{vol}(N_1), \ldots, \operatorname{vol}(N_{r_2})\} \subset S$, where r_2 is the number of complex places of F (and each N_i is a hyperbolic 3-manifold).

In section 4, we provide a counterexample to conjecture 1.3.

1.4. **Exotic volumes.** Recall that for a closed hyperbolic 3-manifold and a representation $\rho : \pi_1(M) \to \mathrm{SL}(n, \mathbb{C})$, Cheeger-Chern-Simons invariant $\widehat{\mathrm{c}}(\rho)$ is given by

$$\widehat{\mathrm{c}}(\rho) = \frac{1}{2}\int_M s^*\left(\operatorname{tr}\left(A \wedge \mathrm{d}A + \frac{2}{3}A \wedge A \wedge A\right)\right) \in \mathbb{C}/4\pi^2\mathbb{Z}, \tag{1.3.1}$$

with E_ρ the flat $\mathrm{SL}(n, \mathbb{C})$-bundle with holonomy ρ, with A the flat connection in E_ρ, and with s a section of E_ρ.

Definition 1.4. For a representation $\rho : \pi_1(M) \to \mathrm{SL}(n, \mathbb{C})$, the **complex volume** $\mathrm{Vol}_{\mathbb{C}}(\rho)$ of ρ is

$$\mathrm{Vol}_{\mathbb{C}}(\rho) = i\,\widehat{\mathrm{c}}(\rho).$$

If ρ is ρ_{geo}, the geometric representation of a hyperbolic 3-manifold M, then

$$\text{Vol}_{\mathbb{C}}(\rho_{\text{geo}}) = \text{vol}(M) + i\,\text{CS}(M),$$

for $\text{CS}(M)$ the Chern-Simons invariant of M.

When ρ is not ρ_{geo}, we call the real part of $\text{Vol}_{\mathbb{C}}(\rho)$ an **exotic volume** of M, to distinguish it from the geometric volume.

By means of the Ptolemy coordinates of [GTZ15], we were able to compute certain exotic volumes of manifolds to at least 50 decimal places of precision, and to express them as linear combinations of geometric volumes of manifolds associated to the same invariant trace field.

Acknowledgments. The authors would like to thank Christian Zickert for guidance and advice, and the 2014 MAPS-REU program at the University of Maryland, led by Kasso Okoudjou, as part of which this work was undertaken.

2. Background

2.1. **Cross-ratios.** It is a feature of hyperbolic geometry that the volume of a complete 3-manifold (if finite) is actually a topological invariant (see e.g. [Ben92, p. 83] for a proof). For an ideal hyperbolic 3-simplex $\Delta = (a, b, c, d)$ defined by four points in $\partial\mathbb{H}^3 \cong \mathbb{C} \cup \{\infty\}$, $\text{vol}(\Delta)$ can be determined knowing just the cross-ratio $[a : b : c : d] = \frac{(c-a)(d-b)}{(d-a)(c-b)}$. Since $\text{Isom}^+(\mathbb{H}^3) \cong \text{PSL}(2, \mathbb{C})$ is 3-transitive, for the purposes of volume calculation we may assume Δ to be of the form $(\infty, 0, 1, z)$, which conveniently has cross-ratio z. The volume of Δ is given by

$$D(\Delta) = \text{Im}\left(\int_0^1 \frac{\log(1-tz)}{t}\,\mathrm{d}t\right) + \arg(1-z)\log|z|. \tag{2.0.1}$$

Given a triangulation of a hyperbolic 3-manifold, one may compute cross-ratios using gluing equations 2.6.1 and 2.7.1. Using cross-ratios, one may compute volumes for each simplex in the triangulation; we refer to section 2.4 for more details. Summing those volumes gives the volume of the manifold: for $\{\Delta_i\}$ the simplices in a triangulation of M,

$$\text{vol}(M) = \sum_i D(\Delta_i). \tag{2.0.2}$$

In our work, we used experimental data to examine relations between the volumes of hyperbolic 3-manifolds which share the same invariant trace field. We begin by briefly reviewing the basics of the algebraic invariants of hyperbolic 3-manifolds relevant to our study.

2.2. The invariant trace field.

Definition 2.1. For a hyperbolic manifold $M = \mathbb{H}^3/\Gamma$ defined by a discrete subgroup Γ of $\text{PSL}(2, \mathbb{C})$, the **trace field** of Γ, denoted $\mathbb{Q}(\text{tr}\,\Gamma)$, is

$$\mathbb{Q}(\{\text{tr}\,\gamma : \pi(\gamma) \in \Gamma\})$$

where $\pi : \text{SL}(2, \mathbb{C}) \to \text{PSL}(2, \mathbb{C})$ is the standard projection map.

Since for any matrices $a, b \in \text{SL}(2, \mathbb{C})$ we have $\text{tr}(aba^{-1}) = \text{tr}(b)$, the trace field of Γ is a conjugation invariant of Γ. Unfortunately, it is not a commensurability invariant, since it is possible to create finite degree extensions of Γ which extend the

trace field: we refer to [MR03, p. 116] for an explicit example. A slight modification smooths over this difficulty.

Definition 2.2. For a non-elementary subgroup $\Gamma \subset \mathrm{PSL}(2,\mathbb{C})$, the **invariant trace field** of Γ is the trace field $\mathbb{Q}(\mathrm{tr}\,\Gamma^{(2)})$, where

$$\Gamma^{(2)} := \langle \gamma^2 \mid \gamma \in \Gamma \rangle.$$

2.3. **The Bloch group.**

Definition 2.3. For any field F, the **Pre-Bloch group on** F, denoted $\mathcal{P}(F)$, is defined as

$$\mathcal{P}(F) = \frac{\langle \{z \in F \mid z \neq 0_F, 1_F\} \rangle}{[z_1] - [z_2] + \left[\frac{z_2}{z_1}\right] - \left[\frac{1-z_2}{1-z_1}\right] + \left[\frac{1-z_2^{-1}}{1-z_1^{-1}}\right]}.$$

The relation in the denominator is known as the **Five Term Relation**. The variables z_1 and z_2 are to be understood as cross-ratios of hyperbolic simplices. The relation encodes that the union of two simplices with volumes $[z_1]$ and $[z_2]$ is also the union of three simplices with volumes $[\frac{z_2}{z_1}]$, $[\frac{1-z_2}{1-z_1}]$, and $[\frac{1-z_2^{-1}}{1-z_1^{-1}}]$. This equivalence is called the Pachner 2-3 move (see figure 1).

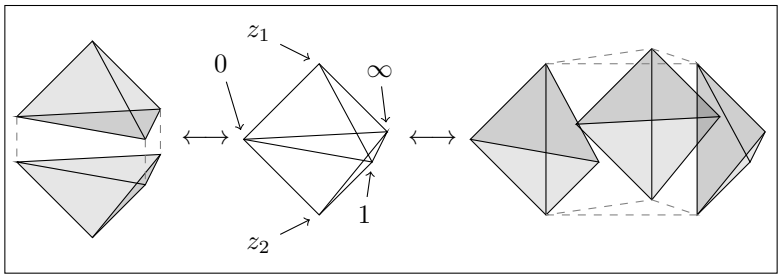

FIGURE 1. The Pachner 2-3 move.

Definition 2.4. For any field F, the **Bloch group on** F, denoted $\mathcal{B}(F)$, is the kernel of the map $d : \mathcal{P}(F) \to F^* \wedge_{\mathbb{Z}} F^*$ defined by

$$d : [z] \mapsto z \wedge (1-z).$$

The map d is an analogue of the Dehn invariant map [Neu98], which (for $F = \mathbb{C}$) fits into an exact sequence of scissors congruence described in e.g. [Dup01]. Thus, understanding $\mathcal{B}(F) = \ker d$ provides insight into scissors congruence groups and generalizations of Hilbert's third problem.

2.4. **Gluing Equations.** Given a hyperbolic 3-manifold M with cusps, the standard procedure for determining $\mathrm{vol}(M)$ is to first triangulate M into a collection of simplices $\{\Delta_i\}$ (together with face pairings), next to compute the cross ratio z_i of each Δ_i, and finally to compute $\mathrm{vol}(M)$ by equation 2.0.2. The first step is well-understood: the manifolds included in the censuses of `SnapPy` include triangulations. The third step is a matter of numerical approximation, but the second step deserves more explanation. We present an overview of the **gluing equations** here, and refer to [NZ85] for a more detailed description, including a treatment of gluing equations for closed manifolds obtained by Dehn surgery.

Given a triangulation $\{\Delta_i\}$ of M, the standard method of finding $\{z_i\}$ is to exploit the torus boundary components and local Euclidean nature of the manifold to produce and solve a system of equations in $\{z_i\}$. Equations 2.6.1, which arise from torus boundary components, are the **cusp equations**, and equations 2.7.1, which arise from local Euclideanness, are the **edge equations**. Together, they are the gluing equations.

Since, in the triangulation of M, a link component appears at the vertices of each simplex, a torus can be determined by truncating the simplices, then making edge identifications to match face identifications, as in figure 2.

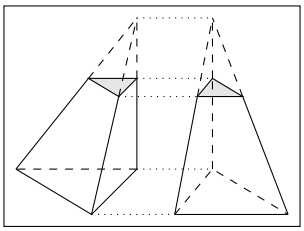

FIGURE 2. Piecing together a torus from a triangulation.

Since the meridian and the longitude of a torus are homotopically circles, it should be possible to require that any path following a meridian or longitude winds exactly once. In other words, it should be possible to construct a system of equations, with variables representing various angles of each Δ_i, such that certain sums are 2π.

By considering each Δ_i as ideal, each segment of such a path can be viewed as complex multiplication (recall that all cross-ratios are in $\mathbb{C} \cup \{\infty\}$. For example, in figure 3, the rotation that takes a point from start to end of a bold arrow is the same rotation that takes 1 to z: multiplication by z. By re-ordering the vertices of Δ_i, other paths may be expressed as re-ordered cross-ratios.

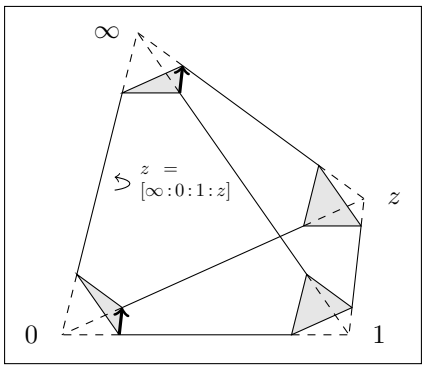

FIGURE 3. Identifying torus traversal with multiplication in $\mathbb{C}$.

Definition 2.5. Let a triangulation be fixed. To each simplex associate a variable z_i. For each edge e_{ij} in the simplex, transforming any point by rotating around

e_{ij} is equivalent to multiplication of that point by either z_i, $\frac{z_i-1}{z_i}$, or $\frac{1}{1-z_i}$ (fix one angle as z_i, determine the rest by cross-ratio rearrangement).

Let p be a closed path in a triangulated surface, transverse to all edges. For every consecutive pair of edges that p crosses, those edges must meet at an angle, which is associated to some z_i, $\frac{z_i-1}{z_i}$, or $\frac{1}{1-z_i}$. The **path monodromy of** p, denoted $\mathcal{M}(p)$, is the product of all these variables.

Definition 2.6. Let a triangulation of a manifold M be fixed. For each torus boundary component T_i of M, choose meridian and longitude paths in the torus (transverse to all edges) m_i and ℓ_i respectively. The **cusp equations** are

$$\mathcal{M}(m_i) = 1 \qquad \text{and} \qquad \mathcal{M}(\ell_i) = 1 \tag{2.6.1}$$

There are two such equations for each torus boundary component.

One more piece of geometric information will be useful. For each edge in the triangulation, consider all face identifications that contain that edge as an axis. Such identifications identify the edges of neighboring faces, and these faces join to form two polygons, one around each vertex of the edge. For example, see figure 4, in which the shaded region is a polygon for the edge shown in bold. We arbitrarily consider the polygon to be the one about the terminus point of the edge.

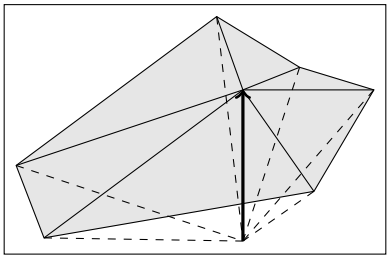

FIGURE 4. Piecing together a polygon from a triangulation.

Definition 2.7. Let a triangulation of a manifold M be fixed. For each distinct edge e_i in the triangulation, let P_i be the polygon described above associated to that edge. Let p_i be a path in P_i circling the central point. The **edge equations** are

$$\mathcal{M}(p_i) = 1 \tag{2.7.1}$$

There are as many edge equations as there are distinct edges in the chosen triangulation.

If two triangulations of M are both composed of non-degenerate, geometrically viable simplices, by Mostow rigidity they must yield the same volume. Therefore, given a triangulation $\{\Delta_i\}$ of M, if the cross-ratios z_i all have positive imaginary part, then computing $\sum_i D(\Delta_i)$ will yield $\mathrm{vol}(M)$. It is possible, however, for a triangulation not to yield solutions that give a geometric volume. In software implementations, this is usually dealt with by re-triangulating using different parameters.

As presented, the system of cusp and edge equations can be hard to solve by hand, because their degree is unbounded. For example, the complement of the knot 6_1 (see figure 5), known as $m032$, has the triangulation given in figure 6, and admits the boundary torus given in figure 7.

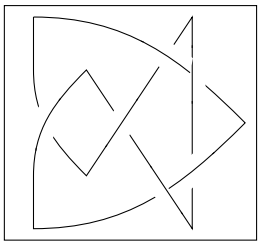

FIGURE 5. 6_1.

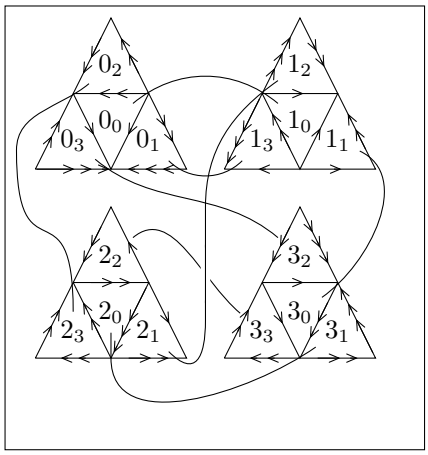

FIGURE 6. $m032$.

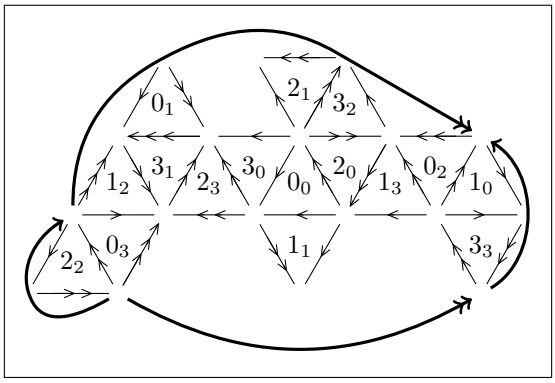

FIGURE 7. The torus boundary of $m032$.

A path through the torus from left to right (for example, from the single-arrow edge of 2_2 to the corresponding edge of 1_0) would have to pass through at least eleven faces, inducing a cusp equation with eleven terms. Computer programs such as `SnapPy` [CDW] can solve these equations (numerically) quite efficiently.

2.5. **Ptolemy coordinates.** The Ptolemy coordinates of Garoufalidis-Thurston-Zickert offer an alternative representation of the information encoded in the gluing and cusp equations. For our purposes, their principal use is encoding information about arbitrary representations $\rho : \pi_1(M) \to \mathrm{PSL}(n, \mathbb{C})$. We refer the reader to [GTZ15], [GGZ15], and present a brief overview here, specialized for the particular case of hyperbolic 3-manifolds.

Definition 2.8. For a fixed triangulation of a manifold M (with vertices labeled 0, 1, 2, 3), a **Ptolemy assignment** is an association of variables in $\mathbb{C}^\times$ to each edge of each simplex satisfying equations 2.8.1 below. We denote the variable of the ith simplex on the edge between vertices j and k as c^i_{jk}.

If two edges are identified, their associated variables are the same. This immediately implies, for example, that $c^i_{jk} = -c^i_{kj}$.

The **Ptolemy relations** are

$$c^i_{03}c^i_{12} + c^i_{01}c^i_{23} = c^i_{02}c^i_{13} \tag{2.8.1}$$

Proposition 2.9. *For a fixed triangulation of a manifold M, and for any Ptolemy assignment of this triangulation,*

$$z_i = \pm\frac{c^i_{03}c^i_{12}}{c^i_{02}c^i_{13}} \tag{2.9.1}$$

where the sign is determined by an obstruction class, as described in [GGZ15] and [GTZ15].

Since in our work we are interested only in z_i, we may often assume without loss of generality that certain $c^i_{jk} = 1$, where the number of such variables depends on the number of cusps of the manifold.

In the case of $m032$ (the manifold presented above), there are only three distinct edges, therefore three independent c^i_{jk} variables. The Ptolemy relations are homogeneous degree 2 equations in two variables, and taking one of the variables to be 1 makes this a readily solvable system.

2.6. **Lattice matching.** Given a large collection of (numerically approximated) hyperbolic 3-manifold volumes (with the same invariant trace field), we desired to construct the coarsest lattice containing the point given by each volume. We desired to reconstruct the linear combination whose sum was the volume of the manifold - we refer to the volume as the projection of the lattice point to $\mathbb{R}$. Searching for representative manifolds of the generating basis of this lattice would then provide insight into the the relation between volumes and the Bloch group. The question we sought to answer therefore was "Given the dimension d of a lattice, as well as a set S of projections of points in that lattice to $\mathbb{R}$, what is a d-subset B of S which, up to a minimal scaling factor, contains all other lattices generated by d-subsets of S?".

2.6.1. *An assumption.* In answering this problem, we had no exact norms: instead of S, we had numerical approximations of elements of S. Using only numerical approximations, we cannot prove that any two elements of S are linearly independent. However, we can be reasonably confident that two numerical representations represent linearly independent elements. In our work, we used upwards of 50 places of precision and used the `LLL` algorithm implemented in `PARI` [GRO14]. If the algorithm indicated that coefficients with magnitude greater than 2^{12} was required to obtain a linear dependence, we considered the two elements linearly independent. As we very rarely observed coefficients with magnitudes greater than 10 and never observed enough linearly independent elements to contradict Borel's result below, we consider this reasonable.

2.6.2. *The lattice dimension.* By a result of Borel [Neu98, p. 397], for an invariant trace field $\mathbb{Q}[x]/\langle p\rangle$, where p has r_2 complex places, $\mathcal{B}(F)/(\text{torsion})$ is isomorphically a lattice in $\mathbb{R}^{r_2}$. We therefore worked under the assumption that $d = r_2$. In some case, we observed strictly less than r_2 linearly independent volumes; we believe this is due to insufficient data, and that given unlimited resources we would eventually discover another, linearly independent volume.

2.6.3. *An example.* Suppose $d = 2$, and we wish to obtain a B for the following (numerical approximations of) S:

$$\begin{aligned} V &= 2.7182818284590 && (\approx e) \\ W &= 5.4365636569180 && (\approx 2e) \\ X &= 6.3496623769612 && (\approx 15\pi - 15e) \\ Y &= 11.7197489640976 && (\approx 2\pi + 2e) \\ Z &= 21.1445269248670 && (\approx 5\pi + 2e). \end{aligned}$$

The coarsest lattice generated by V, W, X, Y, Z may be generated by π and e. We cannot obtain a 2 element subset which generates this lattice, but we would like to recover something close, ideally containing V. We would also like to obtain a measure of how much this 2 element subset B fails to completely generate S.

Definition 2.10. For a d-subset B of S, as described above, the **fit ratio** of B is the smallest positive integer f such that the lattice with generators B contains fS. If no such integer exists, the fit ratio of B is ∞.

We certainly do not wish to select the two smallest elements of S: in the example $\{V, W\}$ has fit ratio ∞. Nor is it sufficient to simply select the two least linearly independent elements: $\{V, X\}$ has fit ratio 15 by considering Y.

A good choice would be $B = \{V, Y\}$, with fit ratio 2. Our algorithm for detecting such B is formalized in algorithm 1, which is implemented in our experimentation software.

2.6.4. *An algorithm.* To find a good choice of B, we first find some linearly independent basis of S (by brute force, if necessary), then express each element of S in terms of that basis, yielding vectors in $\mathbb{Q}^d$ (if this could not be achieved, it would be a contradiction of Borel's result). We then test all d-sized sets of vectors, and select the one with the least determinant. The ratio of this determinant to the fractional GCD of all such determinants yields the fit ratio.

In our implementation, we use `PARI` for the `lindep` algorithm, and as noted in 2.6.1, we use a combination of high precision and detection of large coefficients to determine linear dependence.

Applied to the example, `rational_vecs` is calculated as

$$\left\{(V,(1,0)),(X,(0,1)),(Y,(\frac{1}{4},-\frac{2}{15})),(Z,(-7,-\frac{1}{3}))\right\},$$

discarding W since it is a linear multiple of V. Calculating determininants of potential bases gives:

$$\begin{aligned} \{V,X\} &\to \det\begin{bmatrix}1 & 0\\ 0 & 1\end{bmatrix} = 1 & \{V,Y\} &\to \det\begin{bmatrix}1 & 4\\ 0 & -\frac{2}{15}\end{bmatrix} = -\frac{2}{15} \\ \{V,Z\} &\to \det\begin{bmatrix}1 & -7\\ 0 & -\frac{1}{3}\end{bmatrix} = -\frac{1}{3} & \{X,Y\} &\to \det\begin{bmatrix}0 & 4\\ 1 & -\frac{2}{15}\end{bmatrix} = 4 \\ \{X,Z\} &\to \det\begin{bmatrix}0 & -7\\ 1 & -\frac{1}{3}\end{bmatrix} = 7 & \{Y,Z\} &\to \det\begin{bmatrix}4 & -7\\ -\frac{2}{15} & -\frac{1}{3}\end{bmatrix} = -\frac{34}{15}. \end{aligned}$$

Since $\frac{2}{15}$ is the smallest absolute value of all possible determinants, $B = \{V, Y\}$ is returned by the algorithm. Since the fractional GCD of all possible determinants is $\frac{1}{15}$, the fit ratio of B is 2.

Algorithm 1 Best-fit lattice matching algorithm.

$manifolds \leftarrow$ SORT_BY_INCREASING_VOLUME($manifolds$)
$next_i \leftarrow 2$ ▷ Which e_i we seek a manifold for
$rational_vecs \leftarrow \{(manifolds_1, e_1)\}$ ▷ Tuples (M, v), with $v \in \mathbb{Q}^n$
$rational_basis \leftarrow \{manifolds_1\}$ ▷ All M associated to some e_i
for all $M \in manifolds$ except $manifolds_1$ **do**
  $dep =$ LINDEP(vol$(M), rational_basis)$ ▷ Via PARI; $\langle dep, volumes\rangle = 0$
  if dep shows vol(M) is not a linear combination of others **then**
    if dep shows vol(M) is a rational combination of others **then**
      $rational_vecs \leftarrow rational_vecs \cup \{(M), dep_1^{-1} dep_{2,3,\ldots,n+1}\}$
    else
      if $next_i > n$ **then**
        return Failure ▷ There are more than n l.i. manifolds
      end if
      $rational_basis \leftarrow rational_basis \cup \{M\}$
      $rational_vecs \leftarrow rational_vecs \cup \{(M), e_{next_i}\}$
      $next_i \leftarrow next_i + 1$
    end if
  end if
end for
$gcd \leftarrow \infty$
$best_det \leftarrow \infty$
$best_basis \leftarrow \varnothing$
for all $B \subseteq rational_vecs$ with $|B| = n$ **do**
  $det \leftarrow \det(\{v \mid (M, v) \in B\})$
  if $det \neq 0$ **then**
    $gcd \leftarrow$ fractional_gcd(gcd, det)
    if $det < best_det$ **then**
      $best_det \leftarrow det$
      $best_basis \leftarrow B$
    end if
  end if
end for
return (basis, fit ratio) := $(best_basis, \frac{best_det}{gcd})$

3. Experimentation

Our main results are the following data.

For our work, we used the volumes for a large number of hyperbolic 3-manifolds, which we obtained by performing Dehn surgery on manifolds from a base census. We used `SnapPy` [CDW], although for invariant trace field calculations we used the older `Snap` [Goo] interface.

3.1. **Manifold generation.** The code we used to collect manifold information can be found at `https://github.com/s-gilles/maps-reu-code`. We considered all orientable, cusped, hyperbolic manifolds which can be triangulated using 9 tetrahedra or less (the `OrientableCuspedCensus` within `SnapPy` at the time of work), as well as all link complements using 3 crossings or more (a subset of

`LinkExteriors`). We also considered additional manifolds in the `LinkExteriors` and `HTLinkExteriors` collections.

Of these manifolds, we performed Dehn surgery of type (p, q) over each of the n cusps, with $p \in [0, L(n)]$ and $q \in [-L(n), L(n)]$, (and $(p, q) = 1$) where $L(n)$ is given by figure 8.

$L(n)$	16	12	8	6	4	3	3	2
n	1	2	3	4	5	6	7	≥ 8

FIGURE 8. $L(n)$

Of the resulting manifolds, we discarded those whose invariant trace field resulted in a polynomial with degree 9 or more (or if `SnapPy` or `Snap` were unable to triangulate the result). For each remaining manifold, we we stored intermediate information about the manifold. The resulting file, available at `http://www.curve.unhyperbolic.org/linComb/finalized_data/volumes/all_volumes.csv`, contains over 790,000 manifolds, representing over 6,300 distinct invariant trace fields, with volumes accurate to at least 50 decimal places. The work was performed on the University of Maryland's computation cluster.

3.2. **Lattice matching.** With the data stored in `all_volumes.csv`, we have enough data to conjecture partial lattice generators for 5,900 invariant trace fields. Of those, for 312 invariant trace fields we have enough data to conjecture not only generating volumes for the full lattice, but also representative manifolds associated to the invariant trace field which exhibit those volumes. This data can be found at `http://www.curve.unhyperbolic.org/linComb/finalized_data/volume_spans.csv`, and the code we used for conjecturing lattice generators is available at `https://github.com/s-gilles/maps-reu-code`, an implementation of algorithm 1.

Sample data can be found in section 6.

3.3. **Linear combinations for exotic volumes.** While we used the Ptolemy coordinates for computing volumes of hyperbolic 3-manifolds, the computations may be generalized to compute the volume of any representation $\rho : \Gamma \to \mathrm{PSL}(n, \mathbb{C})$.

The extended Bloch group is exactly the Bloch group up to torsion, so another method for experimentally testing conjecture 1.1 is to produce linear combinations of hyperbolic volumes matching exotic volumes, where these exotic volumes arise from generalized representations into $\mathrm{PSL}(n, \mathbb{C})$ where n is not necessarily 2.

Using the data of `all_volumes.csv`, we have been able to find a great many such combinations. This data is available at `http://www.curve.unhyperbolic.org/linComb/finalized_data/linear_combinations/`.

Sample data can be found in section 6.

4. A counter-example to conjecture 1.3

A secondary result of our work is a counter-example to conjecture 1.3. Assuming the conjecture holds, two of the manfold volumes catologued would imply the existence of a manifold with an impossibly small volume.

Theorem 4.1 ([GMM09, Corollary 1.3])**.** *The Weeks manifold is the unique closed orientable hyperbolic 3-manifold of smallest volume:* $0.9427\ldots$.

Counter-example 4.2. *Conjecture 1.3 is false.*

Proof. The polynomial $p(x) = x^3 - x^2 + 1$ has exactly one complex place. The manifold $m003(2,1)$ has hyperbolic volume $0.9427\ldots$, and the manifold $10^2_{94}(2,3)(5,11)$ has hyperbolic volume $1.4140\ldots$.

If conjecture 1.3 were true, the volumes of these manifolds (which have invariant trace field $\mathbb{Q}[x]/\langle p\rangle$) would be expressable as a linear combination of one generator: $\mathrm{vol}(M)$. Then

$$\mathrm{vol}(M) \mid \frac{0.9427\ldots}{2} = (vol(10^2_{94}(2,3)(5,11)) - \mathrm{vol}(m003(2,1))).$$

This would contradict theorem 4.1. □

In our entire census, we did not observe any counterexamples where the obstruction factor was less than $\frac{1}{2}$. We suspect this is related to the following theorem of Neumann.

Theorem 4.3 ([Neu11, Theorem 2.7])**.** *If M has cusps then $[M]$ is defined in $\mathcal{B}(F)$, for F the invariant trace field of M, while if M is closed $2[M]$ is defined in $\mathcal{B}(F)$.*

5. Evidence for conjecture 1.2

Our data provides an opportunity for examining the strength of conjecture 1.2. It is known that every field with one complex place arises as the invariant trace field of a hyperbolic manifold [MR03], but an open question in general [Neu11].

5.1. **Examples of missing fields.** Our data is necessarily incomplete. Some interesting absences:

(1) Some fields associated to "simple" polynomials such as $x^4 - 2x^2 + 4$, $x^4 + 9$, and $x^7 - 3$ do not arise. This also includes some degree 2 polynomials such as $x^2 + 13$, $x^2 + 22$, and $x^2 - x + 17$, even though it is known that all fields with one complex place must be exhibited by some manifold.

(2) Some number fields, such as the two concrete number fields arising from $\mathbb{Q}[x]/\langle x^4 - x + 2\rangle$, produced surprisingly little data.

For the concrete number field associated to root $-0.850\ldots \pm 1.01\ldots i$, we observed only two volumes: $21.531\ldots$ and $16.383\ldots$. These two volumes are linearly independent, but we know very little about the proposed lattice.

For the concrete number field associated to root $0.850\ldots \pm 0.654\ldots i$, we only observed one volume: $9.054\ldots$, though the lattice should be of dimension 2. This is (from some perspective) the simplest example from our data which does not support conjecture 1.1.

5.2. **Data analysis.** By comparing the fields we observed (under some reasonable restrictions) to a proven-complete census under the same restrictions, we obtain an estimate of the probability that an arbitrary field (within these restrictions) appears in our census. If conjecture 1.2 holds, then our census samples from all possible fields. If our sample was uniformly random, we would then expect that our census contains the same percentage of fields with $r_2 = 1$ as for $r_2 \neq 1$.

For our calculations, we used a online census [JR14] of abstract number fields expressed as polynomials. For the field restrictions we used, this census has been proven complete. In figures 9 and 10, n refers to the degree of the polynomial p to which the field is associated, and D is the discriminant of the polynomial. We

only consider restrictions for which multiple values of r_2 are possible, and we ignore $r_2 = 4$ due to relative scarcity of data (the total fields for $r_2 = 4$ are so numerous that our results are scarce enough to be statistical noise).

Restrictions		$r_2 = 1$			$r_2 = 2$			$r_2 = 3$		
n	$\lvert D\rvert^{1/n}$	Found	Total	%	Found	Total	%	Found	Total	%
4	≤ 8	56	137	40.8%	76	408	18.6%			
4	≤ 10	65	444	14.6%	82	1100	7.4%			
4	≤ 12	66	1056	6.2%	84	2550	3.2%			
4	≤ 15	66	3069	2.1%	84	6728	1.2%			
5	≤ 8	47	77	61.0%	226	736	30.7%			
5	≤ 10	65	472	13.7%	326	3470	9.3%			
5	≤ 12	73	1670	4.3%	356	10992	3.2%			
5	≤ 15	76	7556	1.0%	362	41776	.8%			
6	≤ 8	11	40	27.5%	180	1222	14.7%	166	1851	8.9%
6	≤ 10	28	405	6.9%	374	8434	4.4%	291	10887	2.6%
6	≤ 12	37	2335	1.5%	514	38722	1.3%	352	42123	.8%
6	≤ 15	48	15556	.3%	578	204108	.2%	380	190995	.1%
7	≤ 10	10	137	7.2%	276	8070	3.4%	391	38103	1.0%
7	≤ 12	14	1473	.9%	455	57292	.7%	637	219879	.2%
7	≤ 15	30	16759	.1%	599	506188	.1%	890	1612152	.0%
8	≤ 10	1	22	4.5%	75	752	9.9%	288	3141	9.1%
8	≤ 12	7	246	2.8%	199	5808	3.4%	584	16764	3.4%
8	≤ 15	11	2560	.4%	383	50268	.7%	976	120111	.8%

FIGURE 9. Observed concrete field percentages by restriction

Restrictions		$r_2 = 1$			$r_2 = 2$			$r_2 = 3$		
n	$\lvert D\rvert^{1/n}$	Found	Total	%	Found	Total	%	Found	Total	%
4	≤ 8	56	137	40.8%	60	204	29.4%			
4	≤ 10	65	444	14.6%	66	550	12.0%			
4	≤ 12	66	1056	6.2%	68	1275	5.3%			
4	≤ 15	66	3069	2.1%	68	3364	2.0%			
5	≤ 8	47	77	61.0%	168	368	45.6%			
5	≤ 10	65	472	13.7%	264	1735	15.2%			
5	≤ 12	73	1670	4.3%	294	5496	5.3%			
5	≤ 15	76	7556	1.0%	300	20888	1.4%			
6	≤ 8	11	40	27.5%	162	611	26.5%	143	617	23.1%
6	≤ 10	28	405	6.9%	350	4217	8.2%	263	3629	7.2%
6	≤ 12	37	2335	1.5%	489	19361	2.5%	324	14041	2.3%
6	≤ 15	48	15556	.3%	553	102054	.5%	352	63665	.5%
7	≤ 10	10	137	7.2%	271	4035	6.7%	383	12701	3.0%
7	≤ 12	14	1473	.9%	450	28646	1.5%	629	73293	.8%
7	≤ 15	30	16759	.1%	594	253094	.2%	882	537384	.1%
8	≤ 10	1	22	4.5%	75	376	19.9%	286	1047	27.3%
8	≤ 12	7	246	2.8%	199	2904	6.8%	582	5588	10.4%
8	≤ 15	11	2560	.4%	383	25134	1.5%	974	40037	2.4%

FIGURE 10. Observed abstract field percentages by restriction

Figure 9 implies, in general, a negative correlation between the number of complex places of the field and the probability that it is exhibited by some manifold. Figure 10 offers hope for an explanation.

While figure 9 lists the observed percentage of concrete number fields, figure 10 lists the observed percentage of fields considered as $\mathbb{Q}[x]/\langle p\rangle$: in particular, we treat any two concrete fields arising from different roots of the same polynomial as identical. The percentages are relatively even across rows in this case, which supports that our census was selecting from all possible abstract number fields. This partially supports conjecture 1.2, and more solidly supports the following weaker version.

Conjecture 5.1. *Every non-real abstract number field $\mathbb{Q}[x]/\langle p\rangle$ arises as abstract number field associated to the invariant trace field of some hyperbolic manifold.*

6. Selected examples

We present a selection of lattices, together with the manifolds which may be generators. These are constructed from the `volume_spans.csv` and `linear_combinations` files of our results.

Each of the following lattices are two-dimensional: each is associated to a polynomial with two complex places. Our results contain data for three and even four complex places, but these are harder to represent visually. In the following graphs, one potential generator is arbitrarily assigned to the x-axis, and the other to the y-axis. A point at position (x, y) represents a volume $v = a\,\mathrm{vol}(g_1) + b\,\mathrm{vol}(g_2)$, where $x = a\,\mathrm{vol}(g_1)$ and $y = b\,\mathrm{vol}\,g_2)$.

The gray dots indicate our predicted lattice (based on the volumes of all manifolds associated to that invariant trace field), while the crosses indicate manifolds we have observed: blue + markers indicate geometric volumes, while red $\times$ markers indicate exotic volumes. The relevant volume (whether geometric or exotic) of the manifold is the projection to $\mathbb{R}$ of the point in the lattice.

Figure 11 represents a typical "good" lattice from our data. We obtained a substantial number of distinct volumes (each volume is recorded many times in our census), and we have a number of pairs of volumes which differ by exactly one of our conjectured basis elements.

Figure 12 represents a typical "almost good" lattice from our data. Our fit ratio is 2, which points out that we are unable to fit the exotic volumes of $v2489$ and $t09825$ (either of them) completely into our lattice. Nonetheless, this lattice allows us to conjecture the existence of smaller manifolds which would "fix" this lattice. For example, we might suppose that the nearby exotic volumes of $v2489$ and $t09825$ differ by a generator (or, perhaps, a multiple of a generator): this would imply the existence of a manifold with volume $\frac{\mathrm{vol}(v3318)}{2} \approx 3.2253$ (this is by no means the only volume which would "fix" the lattice).

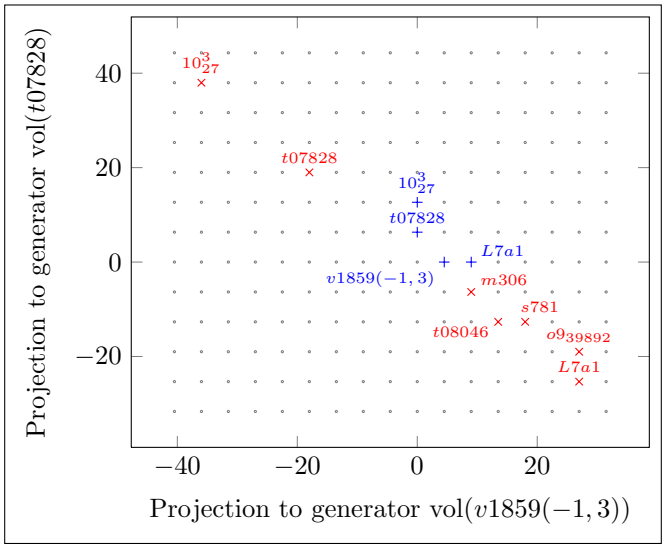

Manifold	Volume	Type	As linear combination
$v1859(-1,3)$	4.4986...	geometric	$1 \cdot \mathrm{vol}(v1859(-1,3)) + 0 \cdot \mathrm{vol}(t07828)$
$t07828$	6.3306...	geometric	$0 \cdot \mathrm{vol}(v1859(-1,3)) + 1 \cdot \mathrm{vol}(t07828)$
$L7a1$	8.9973...	geometric	$2 \cdot \mathrm{vol}(v1859(-1,3)) + 0 \cdot \mathrm{vol}(t07828)$
10^3_{27}	12.661...	geometric	$0 \cdot \mathrm{vol}(v1859(-1,3)) + 2 \cdot \mathrm{vol}(t07828)$
$m306$	2.6667...	exotic	$2 \cdot \mathrm{vol}(v1859(-1,3)) - 1 \cdot \mathrm{vol}(t07828)$
$s781$	5.3334...	exotic	$4 \cdot \mathrm{vol}(v1859(-1,3)) - 2 \cdot \mathrm{vol}(t07828)$
$o9_{39892}$	8.0002...	exotic	$6 \cdot \mathrm{vol}(v1859(-1,3)) - 3 \cdot \mathrm{vol}(t07828)$
10^3_{27}	1.9942...	exotic	$-8 \cdot \mathrm{vol}(v1859(-1,3)) + 6 \cdot \mathrm{vol}(t07828)$
$L7a1$	1.6696...	exotic	$6 \cdot \mathrm{vol}(v1859(-1,3)) - 4 \cdot \mathrm{vol}(t07828)$
$t07828$	0.9971...	exotic	$-4 \cdot \mathrm{vol}(v1859(-1,3)) + 3 \cdot \mathrm{vol}(t07828)$
$t08046$	0.8348...	exotic	$3 \cdot \mathrm{vol}(v1859(-1,3)) - 2 \cdot \mathrm{vol}(t07828)$

FIGURE 11. $p(x) = x^4 - 3x^2 + 4$, root $-1.322... + 0.5i$, prospective basis: $\mathrm{vol}(v1859(-1,3))$, $\mathrm{vol}(t07828)$ with fit ratio 1.

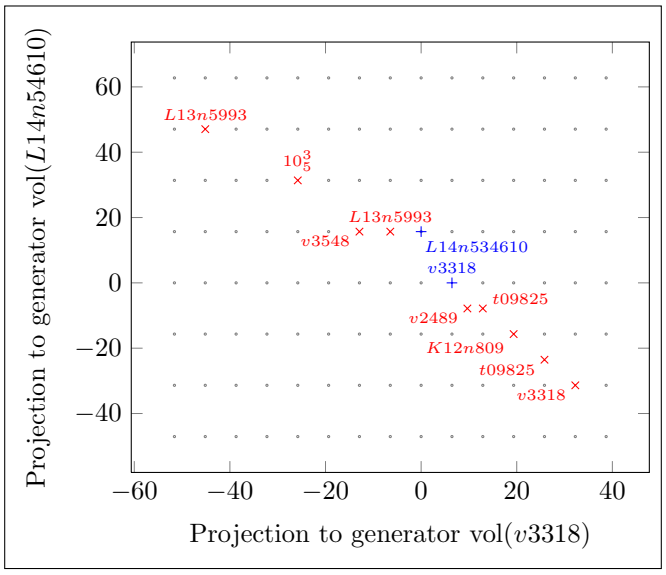

Manifold	Volume	Type	As linear combination
$v3318$	$6.4506\ldots$	geometric	$1 \cdot \mathrm{vol}(v3318) + 0 \cdot \mathrm{vol}(L14n54610)$
$L14n534610$	$15.6881\ldots$	geometric	$0 \cdot \mathrm{vol}(v3318) + 1 \cdot \mathrm{vol}(L14n54610)$
$t09825$	$2.2704\ldots$	exotic	$4 \cdot \mathrm{vol}(v3318) - 1.5 \cdot \mathrm{vol}(L14n54610)$
$v3318$	$0.8770\ldots$	exotic	$5 \cdot \mathrm{vol}(v3318) - 2 \cdot \mathrm{vol}(L14n54610)$
10^3_5	$5.5736\ldots$	exotic	$-4 \cdot \mathrm{vol}(v3318) + 2 \cdot \mathrm{vol}(L14n54610)$
$L13n5993$	$1.9097\ldots$	exotic	$-7 \cdot \mathrm{vol}(v3318) + 3 \cdot \mathrm{vol}(L14n54610)$
$K12n809$	$3.6638\ldots$	exotic	$3 \cdot \mathrm{vol}(v3318) - 1 \cdot \mathrm{vol}(L14n54610)$
$L13n5993$	$9.2374\ldots$	exotic	$-1 \cdot \mathrm{vol}(v3318) + 1 \cdot \mathrm{vol}(L14n54610)$
$v2489$	$1.8319\ldots$	exotic	$1.5 \cdot \mathrm{vol}(v3318) - 0.5 \cdot \mathrm{vol}(L14n54610)$
$t09825$	$5.0572\ldots$	exotic	$2 \cdot \mathrm{vol}(v3318) - 0.5 \cdot \mathrm{vol}(L14n54610)$
$v3548$	$2.7868\ldots$	exotic	$-2 \cdot \mathrm{vol}(v3318) + 1 \cdot \mathrm{vol}(L14n54610)$

FIGURE 12. $p(x) = x^4 + x^2 - 2x + 1$, root $-0.624\ldots + 1.300\ldots i$, prospective basis: $\mathrm{vol}(v3318)$, $\mathrm{vol}(L14n54610)$ with fit ratio 2.

References

[Ben92] R. Benedetti. *Lectures on Hyperbolic Geometry*. Berlin, Heidelberg: Springer Berlin Heidelberg, 1992. ISBN: 978-3-642-58158-8.

[CDW] Marc Culler, Nathan Dunfield, and Jeffrey Weeks. *SnapPy*. URL: `http://www.math.uic.edu/t3m/SnapPy/`.

[Dup01] Johan Dupont. *Scissors congruences, group homology and characteristic classes*. Singapore River Edge, NJ: World Scientific, 2001. ISBN: 978-9810245085.

[GGZ15] Stavros Garoufalidis, Matthias Goerner, and Christian K. Zickert. "The Ptolemy field of 3-manifold-representations". In: *Algebraic & Geometric Topology* 15 (1 2015), pp. 371–397. arXiv:`arXiv:1401.5542`.

[GMM09] David Gabai, Robert Meyerhoff, and Peter Milley. "Minimum volume cusped hyperbolic three-manifolds". In: *J. Amer. Math. Soc.* 22.4 (2009), pp. 1157–1215. ISSN: 0894-0347. eprint: `arXiv:0705.4325`.

[Goo] Oliver Goodman. *Snap*. URL: `http://snap-pari.sourceforge.net/`.

[GRO14] The PARI GROUP. *PARI/GP version* `2.7.0`. The PARI GROUP. Bordeaux, 2014. URL: `http://pari.math.u-bordeaux.fr/`.

[GTZ15] Stavros Garoufalidis, Dylan P. Thurston, and Christian K. Zickert. "The complex volume of $\mathrm{SL}(n,\mathbb{C})$-representations of 3-manifolds". In: *Duke Math. J.* 164.11 (Aug. 2015), pp. 2099–2160. arXiv:`1111.2828v2`.

[JR14] John W. Jones and David P. Roberts. "A database of number fields". In: *LMS Journal of Computation and Mathematics* 17.1 (Dec. 2014), pp. 595–618. URL: `https://www.cambridge.org/core/article/a-database-of-number-fields/B22C15C2B107CF6C6BBA861D075B6F1C`.

[MR03] Colin Maclachlan and Alan W. Reid. *The Arithmetic of Hyperbolic 3-Manifolds*. New York, NY: Springer New York, 2003. ISBN: 978-1-4419-3122-1.

[Neu11] Walter D. Neumann. "Realizing arithmetic invariants of hyperbolic 3-manifolds". In: *Interactions Between Hyperbolic Geometry, Quantum Topology and Number Theory*. (Columbia University). Ed. by Abhijit Champanerkar et al. Vol. 541. Contemporary Mathematics. American Mathematical Society. July 30, 2011, pp. 233–246. ISBN: 978-0-8218-4960-6. arXiv:`1108.0062v1`.

[Neu98] Walter D. Neumann. "Hilbert's third problem and invariants of 3-manifolds". In: *Geometry and Topology Monographs* 1 (1998), pp. 383–411. ISSN: 1464-8989.

[NZ85] Walter D. Neumann and Don Zagier. "Volumes of hyperbolic three-manifolds". In: *Topology* 24.3 (1985), pp. 307–332. ISSN: 0040-9383.

Mathematics Department, University of Maryland, 4176 Campus Dr., College Park, MD 20742

E-mail address: `sgilles@math.umd.edu`

E-mail address: `peter.huston@otterbein.edu`